Cellular/Molecular

GLOBIN-5-Dependent O_2 Responses Are Regulated by PDL-1/PrBP That Targets Prenylated Soluble Guanylate Cyclases to Dendritic Endings

Einav Gross,[1,2] Zoltan Soltesz,[2] Shigekazu Oda,[2] Veronica Zelmanovich,[1] Zohar Abergel,[1] and Mario de Bono[2]
[1]The Hebrew University of Jerusalem, Faculty of Medicine, IMRIC, Jerusalem, 91120 Israel and [2]MRC Laboratory of Molecular Biology, Francis Crick Avenue, Cambridge CB2 0QH, United Kingdom

Aerobic animals constantly monitor and adapt to changes in O_2 levels. The molecular mechanisms involved in sensing O_2 are, however, incompletely understood. Previous studies showed that a hexacoordinated globin called GLB-5 tunes the dynamic range of O_2-sensing neurons in natural *C. elegans* isolates, but is defective in the N2 lab reference strain (McGrath et al., 2009; Persson et al., 2009). GLB-5 enables a sharp behavioral switch when O_2 changes between 21 and 17%. Here, we show that GLB-5 also confers rapid behavioral and cellular recovery from exposure to hypoxia. Hypoxia reconfigures O_2-evoked Ca^{2+} responses in the URX O_2 sensors, and GLB-5 enables rapid recovery of these responses upon re-oxygenation. Forward genetic screens indicate that GLB-5's effects on O_2 sensing require PDL-1, the *C. elegans* ortholog of mammalian PrBP/PDE6δ protein. In mammals, PDE6δ regulates the traffic and activity of prenylated proteins (Zhang et al., 2004; Norton et al., 2005). PDL-1 promotes localization of GCY-33 and GCY-35, atypical soluble guanylate cyclases that act as O_2 sensors, to the dendritic endings of URX and BAG neurons, where they colocalize with GLB-5. Both GCY-33 and GCY-35 are predicted to be prenylated. Dendritic localization is not essential for GCY-35 to function as an O_2 sensor, but disrupting *pdl-1* alters the URX neuron's O_2 response properties. Functional GLB-5 can restore dendritic localization of GCY-33 in *pdl-1* mutants, suggesting GCY-33 and GLB-5 are in a complex. Our data suggest GLB-5 and the soluble guanylate cyclases operate in close proximity to sculpt O_2 responses.

Key words: ***C. elegans*; globin; hypoxia; oxygen sensing; prenyl binding protein; soluble guanylate cyclase**

Introduction

O_2's importance for respiration, and its destructive potential via ROS, has led animals to evolve behavioral, physiological, and cellular responses to acute and chronic changes in O_2. The O_2-sensing mechanisms mediating these responses are incompletely understood. In mammals changes in O_2 evoke rapid responses in specialized tissues, e.g., the carotid bodies and the pulmonary neuroepithelium (Ward, 2008). Tuning of these O_2 responses varies according to the O_2 tension experienced normally by the tissue. The molecular identity of acute O_2 sensor(s) in different mammalian tissues, however, remains elusive. Whether there is one, or several sensors, and whether different sensors work in concert is uncertain.

A molecular mechanism for O_2 sensing is more clearly delineated in *Caenorhabditis elegans*. This nematode lives in rotting fruit (Kiontke et al., 2011) and can grow in $[O_2]$ ranging from 100 to <0.1% (Van Voorhies and Ward, 2000). Nevertheless, *C. elegans* avoids both 21% O_2 and hypoxia (Gray et al., 2004). Avoidance of 21% O_2 is mediated by atypical O_2-binding soluble guanylate cyclases (GCY): GCY-35/GCY-36 in the AQR, PQR, and URX neurons, and GCY-33/GCY-31 in BAG neurons (Cheung et al., 2004; Gray et al., 2004; Persson et al., 2009; Zimmer et al., 2009; Busch et al., 2012; Couto et al., 2013). High $[O_2]$ stimulates GCY-35/GCY-36 heterodimers, gating a cGMP channel that depolarizes AQR, PQR, and URX; low $[O_2]$ depolarizes BAG by stimulating GCY-33/GCY-31. Remarkably, a neuroglobin, GLB-5, sharpens the O_2 tuning of AQR, PQR, and URX, enabling these neurons to switch from high to low activity over a narrow O_2 range, 21–17% (McGrath et al., 2009; Persson et al., 2009). GLB-5 encodes a two-domain protein with an N-terminal

Received Dec. 19, 2013; revised Sept. 24, 2014; accepted Oct. 17, 2014.

Author contributions: E.G. and M.d.B. designed research; E.G., Z.S., S.O., V.Z., and Z.A. performed research; E.G., Z.S., S.O., V.Z., Z.A., and M.d.B. analyzed data; E.G. and M.d.B. wrote the paper.

Research leading to these results has received funding from the European Research Council under the European Union's Seventh Framework Programme (FP/2007-2013)/ERC Grant Agreement 281844 (to E.G., V.Z., and Z.A.) and 269058 (to M.d.B.) and from a Medical Research Council Career Development Fellowship (to E.G.). We thank K.E. Busch for microfluidic devices and help with microscopy, M. van Breugel for help with Y2H experiments, N.P. Barry for help with confocal microscopy, R. Karni for helpful discussions, G. Kay for critical reading of this manuscript, and members of the de Bono and Gross laboratories for comments and advice. Some strains were provided by the CGC, which is funded by National Institutes of Health Office of Research Infrastructure Programs (P40 OD010440), the *C. elegans* Knockout Consortium, and the National BioResource Project (Japan).

The authors declare no competing financial interests.

This article is freely available online through the *J Neurosci* Author Open Choice option.

Correspondence should be addressed to either of the following: Dr. Mario de Bono, MRC Laboratory of Molecular Biology, Francis Crick Avenue, Cambridge CB2 0QH, UK, E-mail: debono@mrc-lmb.cam.ac.uk; or Dr. Einav Gross, Department of Biochemistry and Molecular Biology, IMRIC, Faculty of Medicine, The Hebrew University of Jerusalem, P.O. Box 12271, Jerusalem, 91120 Israel. E-mail: einavg@ekmd.huji.ac.il.

DOI:10.1523/JNEUROSCI.5368-13.2014

globin domain that, like mammalian neuroglobin and cytoglobin, has a hexacoordinated heme Fe^{2+} (Persson et al., 2009; Hundahl et al., 2013). How hexacoordinated globins generally, and GLB-5 in particular, signal is poorly understood—one scenario is that they engage in ROS signaling.

O_2-sensing enables natural *C. elegans* isolates to escape 21% O_2, accumulate where bacteria is thickest, usually at the lawn border, and to settle on food when O_2 drops to 19% (Busch et al., 2012). During domestication the standard N2 (Bristol) laboratory strain lost these behaviors, due to a gain-of-function mutation in a neuropeptide receptor, *npr-1 F215V*, and a loss-of-function mutation in *glb-5, glb-5* (McGrath et al., 2009; Weber et al., 2010).

Here, we explore the functions of GLB-5 neuroglobin further. Since globins are proposed to protect neurons against hypoxia, we ask whether a functional *glb*-5 allele from a Hawaiian wild strain, *glb-5(Haw)*, alters *C. elegans*' responses to hypoxia/reoxygenation stress. We show that without *glb-5* hypoxia experience strongly attenuates both O_2-evoked Ca^{2+} responses in URX neurons and bordering behavior. GLB-5(Haw)'s ability to influence O_2 responses depends on a prenyl binding protein, PDL-1/PrBP, which promotes traffic of the soluble guanylate cyclases to dendritic endings. Our data suggest GLB-5 and the soluble guanylate cyclases operate in close proximity. However, dendritic localization is not essential for GCY-35/GCY36 to respond to O_2 variation.

Materials and Methods

Strains

These include the following: AX204 *glb-5(Bri) V*; *npr-1*(*ad609*) *X*; AX1891 *glb-5*(*Haw*) *V*; *npr-1*(*ad609*) *X*; CB4856 Hawaiian wild strain; AX1198 *gcy-35*(*ok769*) *I*; *npr-1*(*ad609*) *X*; AX2363 *gcy-33*(*ok232*) *V*; *npr-1*(*ad609*) *X*; AX3450 *pdl-1(db508) II*; *glb-5*(*Haw*) *V*; *npr-1*(*ad609*) *X*; AX3451 *pdl-1(gk157) II*; *glb-5*(*Haw*) *V*; *npr-1*(*ad609*) *X*; AX3452 *pdl-1(gk157) II*; *glb-5*(*Bri*) *V*; *npr-1*(*ad609*) *X*; AX1843 *glb-5(Bri) V; npr-1*(*ad609*) *lin-15*(*n765*) *X*; *dbEx[Pglb-5:glb-5*(*Haw*)*::polycismCherry+ lin-15*(+)*]*; AX2983 *pdl-1(gk157) II*; *glb-5*(*Haw*) *V*; *npr-1*(*ad609*) *X; dbEx[Pgcy-37:pdl-1:: polycismCherry;pF15E11.1::GFP]*; AX2979 *pdl-1(gk157) II*; *glb-5*(*Haw*) *V*; *npr-1*(*ad609*) *X; dbEx[Pglb-5:pdl-1:: polycismCherry; pF15E11.1::GFP]*; AX2974 *pdl-1(gk157) II*; *glb-5*(*Haw*) *V*; *npr-1*(*ad609*) *X; dbEx[Ppdl-1:pdl-1:: polycismCherry; pF15E11.1::GFP]*; AX3012 *pdl-1(gk157) II*; *glb-5*(*Haw*) *V*; *npr-1*(*ad609*) *X; dbEx[Pgcy-33:pdl-1:: polycisGFP; pF15E11.1::mCherry*; AX3001 *pdl-1(gk157) II*; *glb-5*(*Haw*) *V*; *npr-1*(*ad609*) *X; dbEx[Ppdl-1:pdl-1:: GFP]*; AX3003 *pdl-1(gk157) II*; *glb-5*(*Haw*) *V*; *npr-1*(*ad609*) *X; dbEx[Ppdl-1:pdl-1:: GFP; Pgcy-37:sense/antisense GFP]*; AX2981 *gcy-35*(*ok769*) *I*; *npr-1*(*ad609*) *lin-15*(*n765*) *X; dbEx[Pgcy-37:gcy-35::HA GFP polycismCherry]*; AX2982 *glb-5*(*Haw*) *V*; *npr-1*(*ad609*) *X; dbEx[Pgcy-37:sense/antisense cDNA pdl-1+ pF15E11.1:: GFP]*; AX2979 *pdl-1(gk157) II*;*glb-5(Bri)) V; npr-1*(*ad609*); *lin-15*(*n765*) *X*;*dbEx[Pglb-5:glb5*(*Haw*)*::polycismCherry+lin-15*(+)*]*; AX3912 *npr-1* (*ad609*) *X; dbEx[Pglb-5:glb-5*(*Haw*)*::polycismCherry+ pF15E11.1::GFP]*; AX2988 *gcy-33*(*ok232*) *V*; *npr-1*(*ad609*) *X; dbEx[Pglb-5:glb-5*(*Haw*)*:: polycismCherry+ pF15E11.1::GFP]*; AX2991 *pdl-1(gk157) II*;*glb-5*(*Haw*) *V*; *npr-1*(*ad609*) *X; dbEx[Pgcy-33:pdl-1:: polycismCherry;pF15E11.1:: RFP]; dbEx[Pgcy-37:pdl-1::polycismCherry;pF15E11.1::GFP]*; AX2997 *gcy-33*(*ok232*) *V*; *npr-1*(*ad609*) *X; dbEx[Pflp-17:gcy-33::GFP polycism Cherry+ccRFP]*; AX2998 *pdl-1(gk157)II*;*gcy-33*(*ok232*) *V*; *npr-1*(*ad609*) *X*;*dbEx[Pflp-17:gcy-33::GFP polycismCherry+ccRFP]*; AX2995 *glb-5(Bri) V*; *npr-1*(*ad609*) *X; dbEx[Pgcy-37::YC2.60+ccRFP]*; AX2994 *glb-5(Haw) V*;*npr-1*(*ad609*) *X; dbEx[Pgcy-37::YC2.60+ccRFP]*; AX2996 *pdl-1(gk157) II*; *glb-5(Haw)V*; *npr-1*(*ad609*) *X; dbEx[Pgcy-37::YC2.60+ccRFP]*; AX2993 *glb-5(Haw)V*; *npr-1*(*ad609*) *X; dbEx[Pflp-17::YC2.60+pF15E11.1::mCherry]*; AX3432 *glb-5(Bri)V*; *npr-1*(*ad609*) *X; dbEx[Pflp-17::YC2.60+pF15E11.1:: mCherry]*; AX3433 *pdl-1(gk157) II*; *glb-5(Haw) V*; *npr-1*(*ad609*) *X; dbEx [Pflp-17::YC2.60+pF15E11.1::mCherry]*; AX3434 *gcy-33*(*ok232*) *V*; *npr-1* (*ad609*) *X; dbEx[Pflp-17::YC2.60+PF15E11.1::mCherry]*; AX2971 *glb-5(Bri) hif-1(ia4) V; npr-1*(*ad609*) *lin-15*(*n765*) *X*; *dbEx[Pglb-5:glb-5*(*Haw*)*:: polycismCherry+lin-15*(+)*]*; AX3454 *glb-5(Bri) hif-1(ia4) V; npr-1*(*ad609*) *lin-15*(*n765*) *X*; *dbEx[Pglb-5:glb-5*(*Haw*)*::polycismCherry+lin-15*(+)*] dbEx [Pgcy-37::YC2.60+ccRFP]*; EVG125 *pdl-1(gk157) II*; *glb-5(Bri) V*; *npr-1*(*ad609*) *X; Ex[Pflp-17::YC2.60+pF15E11.1::mCherry]*; EVG126 *pdl-1(gk157) II*; *glb-5(Bri) V*; *npr-1*(*ad609*) *X; Ex[Pgcy-37::YC2.60+ccRFP]*; EVG127 *gcy-33(ok232) V*; *npr-1*(*ad609*) *X; Ex[Pgcy-37::YC2.60+ccRFP];* EVG387 *gcy-35(ok769) I*; *glb-5(Haw) V*; *npr-1*(*ad609*) *lin-15*(*n765*) *X; dbEx[Pgcy-37:gcy-35::HA GFP polycismCherry]*; EVG444 *pdl-1 II; glb-5(Haw) gcy-33(ok232) V*; *npr-1*(*ad609*) *X; dbEx[Pflp-17:gcy-33::GFP polycismCherry+ccRFP]*.

Behavioral assays

Bordering experiments were performed by transferring 40 L4 hermaphrodites (grown in 21% O_2 at room temperature, RT) to a 5 cm NGM plate that had been seeded 2 d before with OP50 bacteria. Assay plates were put in 1% O_2 (Coy hypoxia chamber; Coy Lab Products) RT for 3–18 h (as indicated), brought back to 21% O_2, and the percentage of animals bordering calculated after 30 min or longer, as indicated. The bordering index is the fraction of worms found on the bacterial lawn border divided by the total number of worms on the plate, multiplied by 100. To quantify speed 10–15 animals were picked onto a 3.5 cm Petri dish containing NGM agar that was seeded 2 d before with *Escherichia coli* OP50. We placed the Petri dish into a custom-designed Perspex chamber (48 × 48 × 17 mm; w × d × h) containing an inner circular cavity designed to fit the 3.5 cm dish. Two metal pipes provided an inlet and an outlet into the chamber for gas supply. Gas was delivered via silicone tubing using a custom-built computer-controlled manifold. The manifold delivered a constant gas flow of 7 ml/min via gas mass flow controllers (FMA5510; Omega) from gas tanks containing defined O_2:N_2 mixtures (British Oxygen Company), and enabled gas switches to be made at defined times. Behavior was recorded using a Grasshopper 20S4M-C CCD camera (Point Gray Research) mounted onto a Leica dissecting microscope using an appropriate C-mount adapter (Leica) at 2 frames/s. Videos were analyzed using Zentracker, a custom software that tracks the center of mass of each animal and calculates instantaneous speed. The software is available on request.

Ethyl methanesulfonate mutagenesis screen

We mutagenized *glb-5(Haw); npr-1* worms as described previously (Brenner, 1974). Two-hundred and fifty mutagenized P_0 hermaphrodites were divided into 50, 9 cm seeded plates. After 4 d, F1 animals (~6000 gravid hermaphrodites) were divided into 60, 9 cm seeded plates and allowed to lay eggs for 2 h. To kill most of the F1 worms without harming the eggs, 3 × 25 μl drops of chloroform were put on the lid of each plate. After 3 d, we transferred ~250 aggregating L4 worms from each plate to a new seeded plate and incubated them in 1% O_2 for 18–20 h. Then, after a 30 min incubation in 21% O_2, we transferred worms that were not on the bacterial lawn border to new plates, and repeated the assay. Nonbordering worms were singled into 3.5 cm plates. Putative mutants were re-assayed and lines in which we verified phenotypes kept.

Mapping

We mapped *db805* to a 4 Mb genomic interval using single nucleotide polymorphisms (SNPs; Davis et al., 2005). To identify the gene disrupted by *db805*, we prepared amplification-free genomic libraries from *db805* mutant DNA (Kozarewa et al., 2009; Weber et al., 2010) and sequenced them with the Illumina Genome Analyzer II. Sequence analysis was performed as described previously (Davis et al., 2005).

Molecular biology

General molecular manipulations followed standard protocols (Sambrook et al., 1989).

Genotyping. The *pdl-1(db805)* allele was followed by amplifying and sequencing the interval flanking the splice-donor region of exon 3. The *gk157* deletion was followed by PCR using primers that flank the deletion. The *glb-5(Bri)* mutation was tracked by examining the size of PCR fragments amplified with primers that flank the duplication in this allele (Persson et al., 2009). The *npr-1(ad609)* allele was followed by amplifying

the interval containing its associated DNA lesions, and using restriction enzyme digestion to distinguish wild-type and mutant alleles.

pdl-1, gcy-35, and gcy-33 cDNA. We extracted total RNA from N2 worms by vortexing with TRIzol (Life Technologies) and acid-washed glass beads, and purifying using an RNeasy Midi Kit (Qiagen). cDNAs were generated by RT-PCR unless otherwise mentioned (OneStep RT-PCR kit; Qiagen). cDNA of *gcy-33* was amplified from a cDNA clone kindly provided by Y. Kohara. Oligonucleotides were designed using the sequences in Wormbase (http://www.wormbase.org/).

Transgenes. Microinjections were performed as described previously (Mello et al., 1991). Plasmids (2.5–50 ng/μl) were coinjected with fluorescent reporters, and multiple independent lines isolated. In brief, N2 genomic DNA was used to amplify the *pdl-1* gene, including 3 kb of upstream sequences. The genomic fragment was cloned into pPD95.75 (A. Fire, personal communication), and then modified by adding an outron-mCherry fragment to make a polycistronic expression vector, as described previously (Coates and de Bono, 2002; Persson et al., 2009). This expression construct was modified to create other expression constructs. To create a *pdl-1* cDNA expression construct, the genomic part of the *pdl-1* gene was replaced with *pdl-1* cDNA. To create constructs that expressed *pdl-1* in the BAG or AQR, PQR, and URX neurons, the promoter region of *pdl-1* was replaced with the 3.3 kb or the 1.3 kb promoter of *flp-17* and *gcy-37*, respectively. To express *pdl-1* in the BAG, AQR, PQR, and URX neurons, the promoter region of *pdl-1* was replaced with the 3.1 kb promoter of *glb-5.* To generate a functional *pdl-1::GFP* expression construct, the *pdl-1* stop codon was deleted by mutagenesis and sequences encoding GFP inserted instead of the outron-mCherry fragment to create an in-frame translational reporter gene. To create a functional *gcy-35::gfp* expression construct, we inserted the GFP reporter sequences after the codon encoding Ser671, thereby retaining intact N and C termini. Similarly, to create a functional *gcy-33::gfp* expression construct, we inserted the GFP reporter sequences after Ala900. To examine how *hif-1* affected *glb-5* responses to hypoxia, we injected a genomic copy of *glb-5(Haw)* into *hif-1(ia4); npr-1(ad609)* animals.

Imaging strains. To create imaging strains that expressed YC2.60 in the BAG or AQR, PQR, and URX neurons, cDNA for YC2.60 (Nagai et al., 2004) was cloned after the *flp-17* and *gcy-37* promoters, respectively. These constructs were injected into *glb-5(Haw); npr-1(ad609)* hermaphrodites, together with 50 ng/μl *cc::RFP* or *F15E11.1:RFP/F15E11.1:GFP* injection markers, following standard methods (Mello et al., 1991).

Cell-autonomous RNA interference

Cell-specific knockdowns were generated as described previously (Esposito et al., 2007). To knockdown *pdl-1* in the AQR, PQR, and URX neurons, sense and antisense RNA sequences of *pdl-1* were expressed from the *gcy-37* promoter. The sense and antisense PCR-fusion products were coinjected into *glb-5(Haw); npr-1(ad609)* hermaphrodites together with 25 ng/μl of the *F15E11.1:GFP* injection marker. Similarly, PCR fusion products of *pgcy-37::GFP* (sense and antisense) were coinjected into *pdl-1(gk157)*; *glb-5(Haw)*; *npr-1(ad609); Ex[Ppdl-1:pdl-1::GFP]* hermaphrodites together with 25 ng/μl *F15E11.1:RFP* injection marker.

Y2H interaction assays

We used the Matchmaker Gold Yeast two-hybrid system (Clontech Laboratories) to investigate protein interactions with PDL-1. In brief, pdl-1 cDNA was cloned into pGBKT7, transformed into Y2HGold yeast cells, and grown on selective Trp plates (according to the manual from Clontech Laboratories). Positive and negative control vectors, pGBKT7–53 and pGBKT7-Lam, were transformed into Y2HGold yeast cells and grown under the same conditions. The cDNAs of *gcy-35*, *gcy-33*, *ras-1*, *rac-2*, *evl-20*, *rab-3*, *rab-18*, *arl-3*, *arl-13*, and *glb-5(Haw)* were cloned into pGADT7, transformed into yeast strain Y187, and grown on selective -Leu plates. The negative control vector, pGADT7-T, was also transformed into Y2HGold yeast cells and grown under the same conditions. Positive colonies from the -Trp and -Leu plates were mixed with a toothpick on a YPDA plate, and grown at 30°C overnight. Y2HGold/Y187 diploids were streaked onto -Trp/Leu double-selection plates and grown for 3–4 d at 30°C. Colonies were then grown overnight in liquid culture, after which 5 μl of diluted and nondiluted diploid suspensions were put on Trp/Leu/Aureobasidin A/X-α-Gal or -Trp/-Leu/-Ade/-His/Aureobasidin A/X-α-Gal plates. Colony growth was monitored after 3–4 d to detect protein interaction.

Ca^{2+} imaging

Ca^{2+} imaging experiments were performed as described previously (Persson et al., 2009). Ca^{2+} responses were recorded at 2 frames/s using a Zeiss Axio Observer D1 inverted epifluorescence microscope or an Olympus IX71S1F-3–5 inverted microscope equipped with a 40× C-Apochromat lens (Carl Zeiss) or UAPON40X Universal apochromatic water-immersion objective (Olympus) and Optosplit II beam splitter or DV2 2-channel imager (Cairn Research and Photometrics, respectively), Cascade II 1024 EMCCD camera, or Rolera EM-C2 (Photometrics and QImaging, respectively), and MetaMorph software (Molecular Devices). For imaging experiments, we glued the worms to agarose pads (2% agarose in M9) using Dermabond tissue adhesive (Closure Medical). Immobilized worms were trapped inside a 500 μm deep rectangular PDMS chamber. Alternatively, we anesthetized the worms using 10 mM levamisole and put them in a custom-made, airtight microfluidic chamber. Humidified gases were delivered to the microfluidic chambers using a PHD 2000 syringe pump (Harvard Apparatus) at a flow rate of 1 ml/min. Teflon valves, regulated by a ValveBank Controller (Automate Scientific), were used to rapidly switch between gas mixtures. Image analysis was performed using custom-written MATLAB software.

Confocal microscopy

We mounted worms on 2% agarose pads (in M9 buffer supplemented with 10 mM sodium azide), and imaged them on a Zeiss LSM 510 laser scanning confocal microscope using a Plan-Apochromat 63× 1.4 NA objective (Zen operating software; Carl Zeiss). Image analysis was performed using ImageJ (Abramoff et al., 2004).

Results

The neuroglobin GLB-5 regulates *C. elegans* responses to hypoxic exposure

Transcription of many globin genes, including some *C. elegans* globins, is induced by hypoxia (Sun et al., 2001; Hoogewijs et al., 2007). This regulated expression is proposed to protect against hypoxia/re-oxygenation damage (Burmester and Hankeln, 2009). To investigate if GLB-5 altered *C. elegans* responses to hypoxia/re-oxygenation stress, we exposed animals bearing the functional *glb-5(Haw)* allele found in natural isolates or the loss-of-function *glb-5(Bri)* allele found in N2 Bristol lab strain, to 1% O_2, returned them to 21% O_2, and looked for differences in behavior. In our assays we used animals that also carried the *npr-1 215F* allele or the *npr-1(ad609)* functional null allele, since the *npr-1 215V* gain-of-function allele found in N2 suppresses the activity of some O_2-sensing circuits (Gray et al., 2004; Cheung et al., 2005; Rockman and Kruglyak, 2009; Weber et al., 2010). We incubated the *glb-5(Bri); npr-1(ad609)* and *glb-5(Haw); npr-1(ad609)* animals (hereafter referred to as *npr-1* and *glb-5(Haw); npr-1* animals, respectively), and animals from the Hawaiian wild strain CB4856 (bearing the natural *glb-5(Haw)* and *npr-1(215F)* alleles) in 1% O_2 for 3, 6, 9, and 18 h, transferred them to 21% O_2, and examined their behavior after 30 min. When grown in 21% O_2 animals from all three strains gather where the bacteria grow thickest, at the border of the lawn (Fig. 1*A*; de Bono and Bargmann, 1998). Upon exposure to 1% O_2, animals from each strain left the food and accumulated outside the bacteria. When returned to normoxia, *glb-5(Haw); npr-1* and CB4856 animals immediately accumulated at the lawn border, regardless of time in hypoxia. In contrast, *npr-1* animals incubated in hypoxia for 18 h showed little preference for the border when returned to 21% O_2 (Fig. 1*B*). The hypoxia-induced inhibition of bordering was reversed within 4 h of return to normoxia (Fig. 1*C*). Bordering reflects an O_2 preference, with $[O_2]$ ~13% in the thicker bacteria

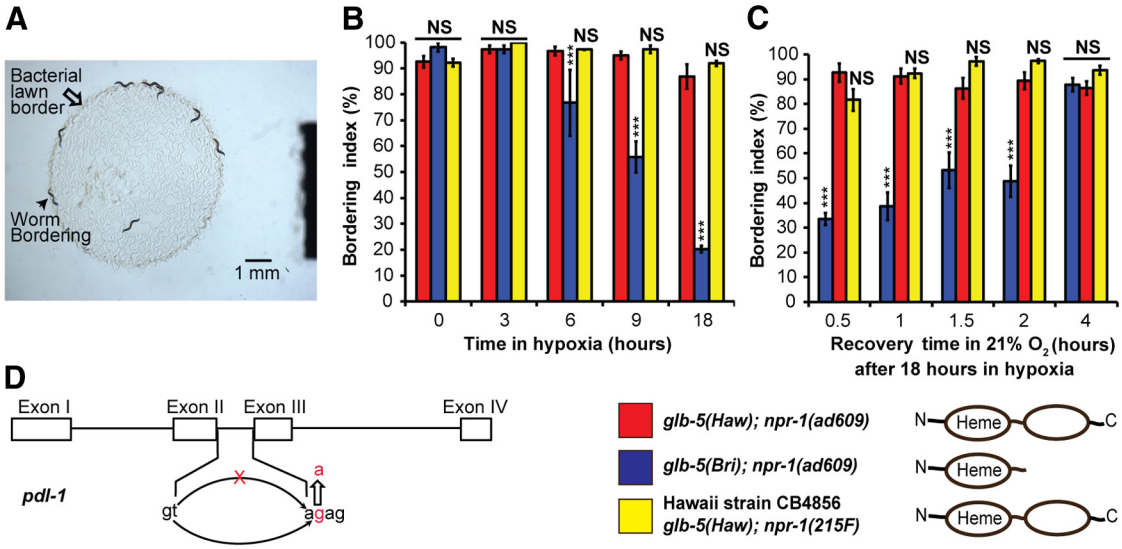

Figure 1. GLB-5(Haw) modifies *C. elegans* responses to hypoxia/re-oxygenation. ***A***, Bordering measures accumulation of animals where the bacterial food lawn grows thickest, at the border. ***B***, Bordering behavior after incubation at 1% O_2 for various lengths of time. Bordering was measured 30 min after animals were returned to 21% O_2. *glb-5(Haw)* is the natural wild allele (yellow and red bars); *glb-5(Bri)* is a loss-of-function allele of *glb-5* (blue bar) selected during domestication that expresses a truncated GLB-5 protein. Asterisks indicate significance compared with *glb-5(Haw); npr-1* animals. ***C***, Time course of recovery of bordering by animals previously exposed to hypoxia. Asterisks indicate significance for comparisons with *glb-5(Haw); npr-1(ad609)* animals. The schematic drawings on the bottom-right corner represent the full-length active GLB-5 (Hawaii) and the truncated nonactive GLB-5(Bri). ***D***, A schematic diagram of *pdl-1*, highlighting the splice acceptor site mutation in the *db805* allele; $n = 4$ or more assays performed over at least 3 d. $^{***}p < 0.001$, Kruskal–Wallis test with Dunn's post-test. Error bars represent SEM.

at the border, and ~17% O_2 at the lawn center (Gray et al., 2004). These results suggest that GLB-5(Haw) signaling enables *C. elegans* exposed to hypoxia and returned to normoxia to remain sensitive to these O_2 differences and to border.

C. elegans PDE6δ/PrBP prenyl binding protein is required for GLB-5 function

How does GLB-5(Haw) alter O_2 sensing? To investigate this question we turned to forward genetics, and sought genes required for *glb-5* signaling. Originally, we identified the *glb-5(Haw)* allele because it enables natural isolates of *C. elegans* to switch from slow to rapid movement on a bacterial lawn when O_2 rises from 17 to 21% (Persson et al., 2009). Although robust, this assay is too labor intensive for forward genetic screens. In contrast, identifying mutations that prevent *glb-5(Haw); npr-1* animals from bordering after hypoxia exposure is amenable to this approach. We mutagenized *glb-5(Haw); npr-1* animals and sought mutants that, after experiencing 1% O_2, failed to border immediately after return to 21% O_2. To exclude mutations that indiscriminately disrupted bordering, we selected lines that resumed bordering after recovering at 21% O_2 for 4 h. We isolated four mutants that satisfied these criteria. By combining Snip SNP mapping with Illumina whole genome sequencing (Wicks et al., 2001; Sarin et al., 2008) we mapped one allele, *db805*, to a 3.8 Mb genomic interval on chromosome II, and identified 10 mutations in this interval. Only one of these mutations altered a predicted open reading frame, disrupting a splice acceptor site in *pdl-1* (Fig. 1*D*). *pdl-1* encodes a 17 kDa protein orthologous to mammalian PDE6δ (phosphodiesterase 6, δ-subunit). PDL-1 and human PDE6δ share 69% amino acid identity at the protein level.

PDE6δ was originally identified as a subunit of PDE6 from bovine retina (Gillespie et al., 1989). Biochemical studies showed that it is a prenyl binding protein (PrBP) that can extract prenylated proteins such as small lipidated GTPases (e.g., Ras) from membranes, sequestering them in the cytoplasm, and facilitating their traffic to different membrane compartments (Chandra et al., 2012). Mice lacking PDE6δ are small but viable; they exhibit progressive cone–rod dystrophy and defective localization of prenylated rhodopsin kinase (GRK1) and PDE6 catalytic subunits to rod outer segments (Zhang et al., 2007).

To confirm the *pdl-1* phenotype, we obtained a deletion allele, *gk157*, which removed most of the *pdl-1* coding region and ~0.5 kb of the upstream promoter region. *pdl-1(gk157)* delayed the recovery of bordering in *glb-5(Haw); npr-1* animals exposed to hypoxia more strongly than the *pdl-1(db805)* mutation (Fig. 2*A*). Since *pdl-1(gk157)* is probably a null allele, we used it in subsequent experiments, unless otherwise indicated.

PDL-1 functions in the same neurons as GLB-5

Where does PDL-1 function to modify GLB-5-dependent behaviors? *glb-5* is expressed in the AQR, PQR, URX, and BAG O_2-sensing neurons. Previous work showed that selectively expressing a *glb-5(Haw)* transgene in AQR, PQR, and URX neurons confers on *npr-1* animals the sharply tuned O_2 responses of *glb-5(Haw); npr-1* animals (McGrath et al., 2009; Persson et al., 2009). To identify where PDL-1 is expressed, we generated a transgene in which genomic DNA for *pdl-1* was fused in-frame with a sequence-encoding GFP (Fig. 2*B*). Using behavioral assays, we showed that this transgene was fully functional (Fig. 2*C*,*F*). We then crossed it with a strain expressing a functional *pglb-5::glb-5(Haw)::mCherry* fusion construct, and looked for colocalization of green and red fluorescence in animals bearing both transgenes. *pdl-1* and *glb-5(Haw)* were coexpressed in the AQR, PQR, URX, and BAG neurons (Fig. 2*B*). *pdl-1* was also expressed in other neurons in the head and tail.

Is PDL-1 generally required for GLB-5(Haw) signaling to modify O_2 sensing, or are its effects specific to the hypoxia paradigm? To address this, we asked whether *pdl-1* mutations affected the ability of normoxia-cultivated *glb-5(Haw); npr-1* animals to switch from rapid movement at 21% O_2 to slow movement at 17% O_2 (McGrath et al., 2009; Persson et al., 2009). Consistent

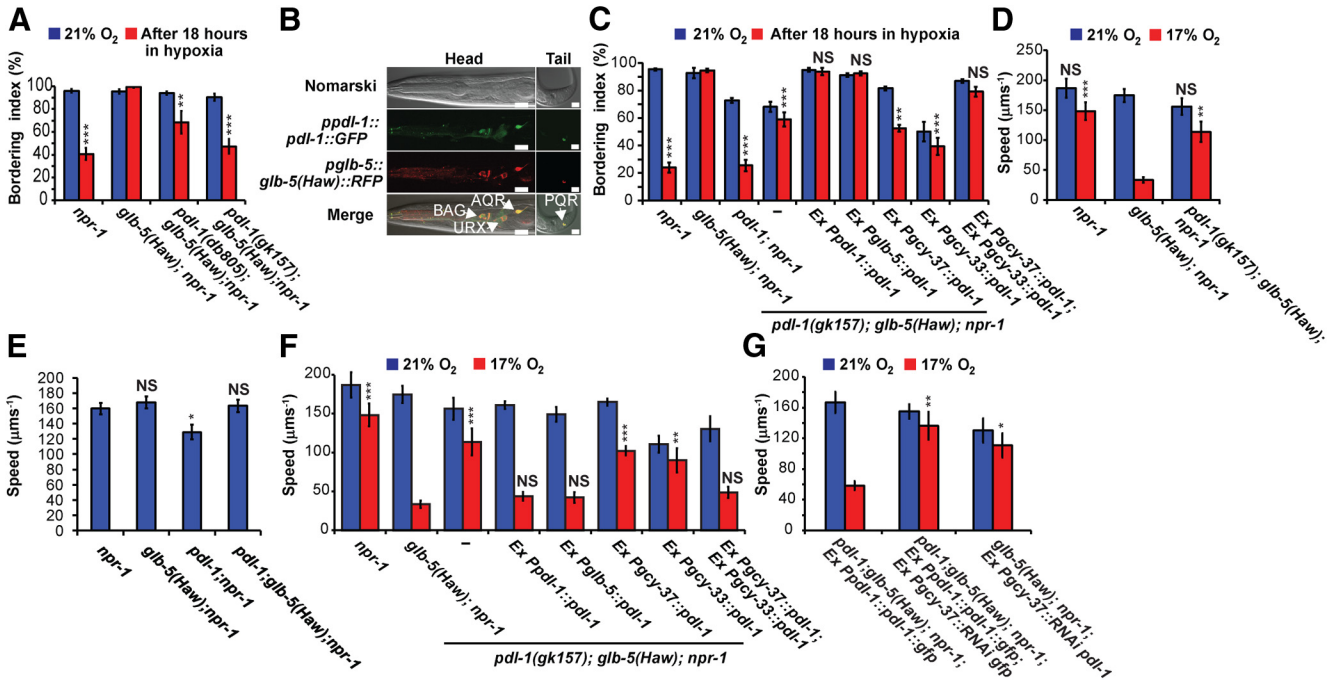

Figure 2. PDL-1 acts in the AQR, PQR, URX, and BAG neurons to promote GLB-5(Haw)-dependent O_2 responses. ***A***, Disrupting *pdl-1* inhibits the rapid recovery of bordering in *glb-5(Haw); npr-1* animals returned to 21% O_2 after exposure to hypoxia. Bordering was measured 30 min after return to 21% O_2. Asterisks indicate significance for comparisons with *glb-5(Haw); npr-1* animals. Kruskal–Wallis test with Dunn's post-test. ***B***, *pdl-1* is strongly expressed in the AQR, PQR, URX, and BAG O_2-sensing neurons, which are highlighted by a *pglb-5::glb-5(Haw)::RFP* fiduciary marker. Scale bars: 10 μm. ***C***, Fast recovery of bordering behavior after prolonged hypoxia requires PDL-1 activity in the AQR, PQR, URX, and BAG neurons. Promoters used for transgenic rescue drive expression in the following: *pglb-5* (AQR, PQR, URX, and BAG); *pdl-1* promoter (multiple neurons); *pgcy-33* (BAG); and *pgcy-37* (AQR, PQR, and URX). Asterisks indicate significance for comparisons to *glb-5(Haw); npr-1* animals after hypoxia treatment. Kruskal–Wallis test with Dunn's post-test. ***D***, PDL-1 is required for GLB-5(Haw) to retune *C. elegans* O_2 sensitivity, and to enable *glb(Haw);npr-1* animals to switch from rapid to slow movement when O_2 drops from 21 to 17%. Asterisks indicate significance for comparisons with *glb-5(Haw); npr-1* at 17% O_2. Kruskal–Wallis test with Dunn's post-test. ***E***, Disrupting *pdl-1* slightly but significantly reduces *C. elegans*' speed of movement at 21% O_2 when *glb-5* is defective. Asterisks indicate significance for comparisons with *npr-1*. One-way ANOVA with Bonferroni's multiple-comparison test. ***F***, PDL-1 functions in O_2-sensing neurons to promote O_2-evoked changes in locomotor behavior; transgenes used are the same as in ***C***. Kruskal–Wallis test with Dunn's post-test. Asterisks indicate significance for comparisons with *glb-5(Haw); npr-1* animals at 17% O_2. ***G***, RNAi knockdown of *pdl-1* in AQR, PQR, and URX suppresses the retuning of O_2 responses mediated by *glb-5(Haw)*. Asterisks indicate significance for comparisons with *pdl-1; glb-5(Haw); npr-1; Ex ppdl-1::pdl-1::gfp* at 17% O_2. Kruskal–Wallis test with Dunn's post-test; $n \geq 4$, $^*p < 0.05$, $^{**}p < 0.01$, and $^{***}p < 0.001$. Error bars represent SEM.

with a general role, *pdl-1; glb-5(Haw); npr-1* animals moved much faster than *glb-5(Haw); npr-1* animals at 17% O_2 (Fig. 2*D*). These data suggest that GLB-5(Haw) effects on O_2 responses depend on correct trafficking of prenylated proteins. Counterintuitively, disrupting *pdl-1* also slightly but significantly reduced the rate of movement of *npr-1* animals at 21% O_2 (Fig. 2*E*), suggesting PDL-1 can influence O_2 sensing independently of GLB-5, perhaps by affecting soluble guanylate cyclases. Does PDL-1 act in the same neurons as GLB-5 to regulate O_2 responses? Replacing the *pdl-1* promoter with the *glb-5* promoter enabled *pdl-1; glb-5(Haw); npr-1* animals exposed to hypoxia to resume bordering rapidly after re-oxygenation, consistent with PDL-1 and GLB-5 functioning in the same cells (Fig. 2*C*). However, expressing *pdl-1* specifically in the AQR, PQR, and URX neurons, by replacing the *pdl-1* promoter with the *gcy-37* promoter, or in BAG neurons, using the *gcy-33* promoter, did not rescue the hypoxia-evoked decrease in bordering (Fig. 2*C*), suggesting *pdl-1* is required in AQR, PQR, URX, and BAG. Consistent with this, coexpressing the p*gcy-33::pdl-1* and p*gcy-37::pdl-1* transgenes rescued bordering behavior after hypoxia (Fig. 2*C*).

PDL-1 also acts in the AQR, PQR, URX, and BAG neurons to enable normoxia-cultivated *glb-5(Haw); npr-1* animals to switch from rapid movement at 21% O_2 to slow movement at 17% O_2. This phenotype could be rescued by expressing *pdl-1* from its own promoter, or from the *glb-5* promoter (Fig. 2*F*). As for bordering behavior, expressing *pdl-1* specifically in the AQR, PQR, and URX neurons, using the *gcy-37* promoter, or only in BAG neurons, using the *gcy-33* promoter, failed to rescue *glb-5(Haw)*-dependent responses to a switch from 21 to 17% O_2. In contrast, coexpressing the two transgenes rescued the behaviors (Fig. 2*F*). To confirm our results, we made RNAi constructs under the control of the *gcy-37* promoter that targeted *pdl-1* or GFP sequences. We injected these into *pdl-1; glb-5(Haw); npr-1* mutant animals that expressed a *pdl-1(cDNA)-GFP* fusion construct from the *pdl-1* promoter. Whereas animals not expressing the RNAi constructs strongly reduced movement when switched from 21 to 17% O_2, animals expressing the RNAi transgenes did not (Fig. 2*G*). These data suggest that PDL-1 acts in AQR, PQR, URX, and BAG neurons to promote *glb-5(Haw)*-dependent O_2 responses in behavioral paradigms that operate at very different timescales.

PDL-1/PrBP mediates localization of soluble guanylate cyclases to dendritic endings

Mammalian PrBP/PDE6δ interacts with prenylated proteins and nonprenylated small GTPases and regulates their traffic (Hanzal-Bayer et al., 2002). GLB-5 is in neither of these categories, but three of the atypical soluble guanylate cyclases required for O_2 responses—GCY-35 and GCY-36 in AQR, PQR and URX neurons, and GCY-33 in BAG neurons—are predicted to have C-terminal -CAAX sequences, suggesting they are prenylated (Cheung et al., 2004, 2005; Gray et al., 2004; Persson et al., 2009;

Zimmer et al., 2009; Busch et al., 2012). These heme proteins are thought to directly bind O_2, andO_2 binding is thought to modulate their cGMP production and to change neural activity by gating cGMP ion channels (Couto et al., 2013). The functional importance of the CAAX motif has been directly tested for the GCY-36 soluble guanylate cyclase. Mutating sequences encoding the CAAX motif to encode SAAX disrupted GCY-36 localization to dendritic endings and resulted in a nonfunctional *gcy-36* gene (Cheung et al., 2004).

To examine if PDL-1 regulates trafficking of GCY-35 and GCY-33, we made transgenes that expressed functional fluorescently tagged versions of these proteins. Tagging GCY-35 N terminally or C terminally interfered with its biological activity. We therefore inserted *gfp* cDNA into sequences encoding a predicted flexible loop in the GCY-35 C-terminal tail. Like GLB-5(Haw), GCY-35-GFP was enriched at the dendritic tips of URX neurons (Fig. 3*A*). Moreover, this transgene largely (although not completely) restored O_2 control of locomotor activity to *gcy-35; npr-1* mutants (Fig. 3*B*). We compared the accumulation of GCY-35::GFP in the dendrite and cell body of URX neurons in *gcy-35; npr-1* and *gcy-35; pdl-1; npr-1* animals (Fig. 3*C*,*D*). While fluorescence in the cell body was very similar in the two genotypes, loss of *pdl-1* essentially abolished GCY-35-GFP accumulation at the tip of URX dendrites. Thus, *pdl-1* is required for correct localization of GCY-35 at dendritic endings. However, localization of GCY-35 to dendrites is not essential for O_2-evoked responses.

We also examined if prolonged exposure to hypoxia (18 h) altered levels and distribution of GCY-35 in the URX neurons. We incubated *gcy-35; npr-1* and *gcy-35; glb-5(Haw); npr-1* animals in 1% or 21% O_2 and quantified GCY-35-GFP fluorescence in dendrites (Fig. 3*E*). Exposure to hypoxia did not change GCY-35 levels in the dendrites of *npr-1* animals or *glb-5(Haw); npr-1* animals. We observed reduced cell body expression of GCY-35::GFP in *glb-5(Haw); npr-1* animals following hypoxia, but this may reflect regulation of transcription from the *gcy-37* promoter (Cheung et al., 2005).

To test if PDL-1 can directly interact with GCY-35, we performed yeast two-hybrid experiments (Y2H). We used PDL-1 as bait, mated it with a prey strain expressing GCY-35, and examined diploid growth on selective plates (Fig. 3*F*). The rapid growth of the *pdl-1/gcy-35* diploids suggested that GCY-35 and PDL-1 physically interact. To determine whether this interaction required prenylation of GCY-35, we disrupted the CAAX prenylation motif by a cysteine-to-serine codon change. PDL-1 failed to interact with this mutant form of GCY-35. These results suggest that PDL-1, like its mammalian counterpart, is a prenyl binding protein involved in protein transport. More specifically, it is required to traffic GCY-35 to the nonciliated dendritic endings of URX by a prenylation-dependent physical interaction.

Mammalian PrBP/PDE6δ can also interact with the nonprenylated Arf-like (Arl) small GTPases, Arl2-GTP and Arl3-GTP. We therefore used the Y2H assay to examine if PDL-1 can also interact with *arl-3* and *arl-13*. No significant growth was observed (Fig. 3*F*). Interestingly, we did observe a weak but reproducible interaction with the *rac-2* GTPase (Fig. 3*F*).

Like GCY-35-GFP, GLB-5(Haw)-mcherry is enriched at the dendritic endings of URX neurons (McGrath et al., 2009; Persson et al., 2009). We therefore tested if GLB-5(Haw)-mcherry localization or expression was also regulated by *pdl-1*. GLB-5(Haw)-mcherry levels were significantly decreased in both URX dendrites and cell bodies (Fig. 3*G*,*H*). Thus, PDL-1 directly or indirectly regulates the expression and/or stability of GLB-5(Haw).

Our expression studies and cell-specific rescue experiments suggested that *pdl-1* functions not only in AQR, PQR, and URX but also in BAG sensory neurons (Fig. 2*C*,*F*). BAG neurons express GCY-33, a soluble guanylate cyclase that also has a C-terminal CAAX prenylation motif. GCY-33::GFP accumulated strongly at the dendritic endings of BAG (Fig. 3*I*). This dendritic fluorescence was reduced in *pdl-1; gcy-33; npr-1* mutants although not abolished (Fig. 3*I*,*J*), suggesting that PDL-1 contributes to but is not solely responsible for localizing GCY-33 to BAG dendritic endings. Levels of GCY-33::GFP in the cell body were not altered in *pdl-1* mutants (Fig. 3*J*).

To test if PDL-1 and GCY-33 can interact directly, we set up Y2H experiments, as described previously for GCY-35. GCY-33/PDL-1-expressing diploids formed detectable but much smaller colonies than GCY-35/PDL-1 diploids, suggesting a weaker interaction. Consistent with this, when we tested the ability of PDL-1/GCY-33 diploids to grow on a more restrictive medium, containing six selectable markers (-Trp/-Leu/-Ade/-His/Aureobasidin A/X-α-Gal), the PDL-1/GCY-33 diploids did not form colonies whereas the GCY-35/PDL-1 diploids did (Fig. 3*F*, button, right). Our results suggest that although GCY-33 localization in BAG dendritic endings is regulated by PDL-1, the interaction between PDL-1 and GCY-33 may involve additional proteins. Moreover, PDL-1-independent pathways exist to traffic GCY-33, since a small but significant amount of GCY-33 is found in BAG dendritic endings even in the absence of PDL-1 (Fig. 3*I*,*J*).

O_2-evoked Ca^{2+} responses in URX in *pdl-1 mutants*

To investigate how loss of *pdl-1* and mislocalization of soluble guanylate cyclases altered the physiology of O_2-sensing neurons, we monitored O_2-evoked responses in these neurons using the Ca^{2+} sensor YC2.60 (Nagai et al., 2004). YC2.60 has higher Ca^{2+} affinity than the YC3.60 sensor we used previously, providing a better readout of intermediate Ca^{2+} levels (Persson et al., 2009; Busch et al., 2012). The ratiometric nature of YC Ca^{2+} sensors permits a steady-state level of Ca^{2+} to be compared across genotypes, which is informative since O_2-sensing neurons signal tonically (Persson et al., 2009; Busch et al., 2012). We began by examining animals grown at normoxia.

We compared Ca^{2+} responses evoked in URX by two O_2 profiles: 21%–17%–21% O_2 and 21%–7%–21% O_2. We included the 21%–7%–21% profile as a control because the neuronal activity of the O_2-sensing neurons and the speed of *npr-1* animals at 7% O_2 is the same regardless of the *glb-5* genotype (Persson et al., 2009). The 21%–17%–21% O_2 stimulus train probes the ability of GLB-5(Haw) to alter the dynamic range of the O_2 response (Fig. 4*A*,*B*; Persson et al., 2009). As expected, the *glb-5(Haw)* allele sharpened the tuning of URX: at 17% O_2 Ca^{2+} was significantly lower in *glb-5(Haw); npr-1* animals compared with *npr-1* animals, and was indistinguishable from Ca^{2+} at 7% O_2 (Fig. 4*A*,*B*). These results mirror the behavioral data: *glb-5(Haw); npr-1* animals switch to slow movement at much higher O_2 levels than *npr-1* animals (Persson et al., 2009). Despite the GCY-35 localization defects, and consistent with our behavioral observations, O_2 stimuli evoked robust Ca^{2+} responses in URX in both *pdl-1; npr-1* and *pdl-1; glb-5(Haw); npr-1* animals (Fig. 4*C*,*D*). However, URX Ca^{2+} at 17% O_2 was significantly higher in *pdl-1; glb-5(Haw); npr-1* compared with *glb-5(Haw)*; *npr-1* (Fig. 4*E*). This correlated with the greater locomotor activity of *pdl-1; glb-5(Haw); npr-1* animals kept at 17% O_2 compared with *glb-*

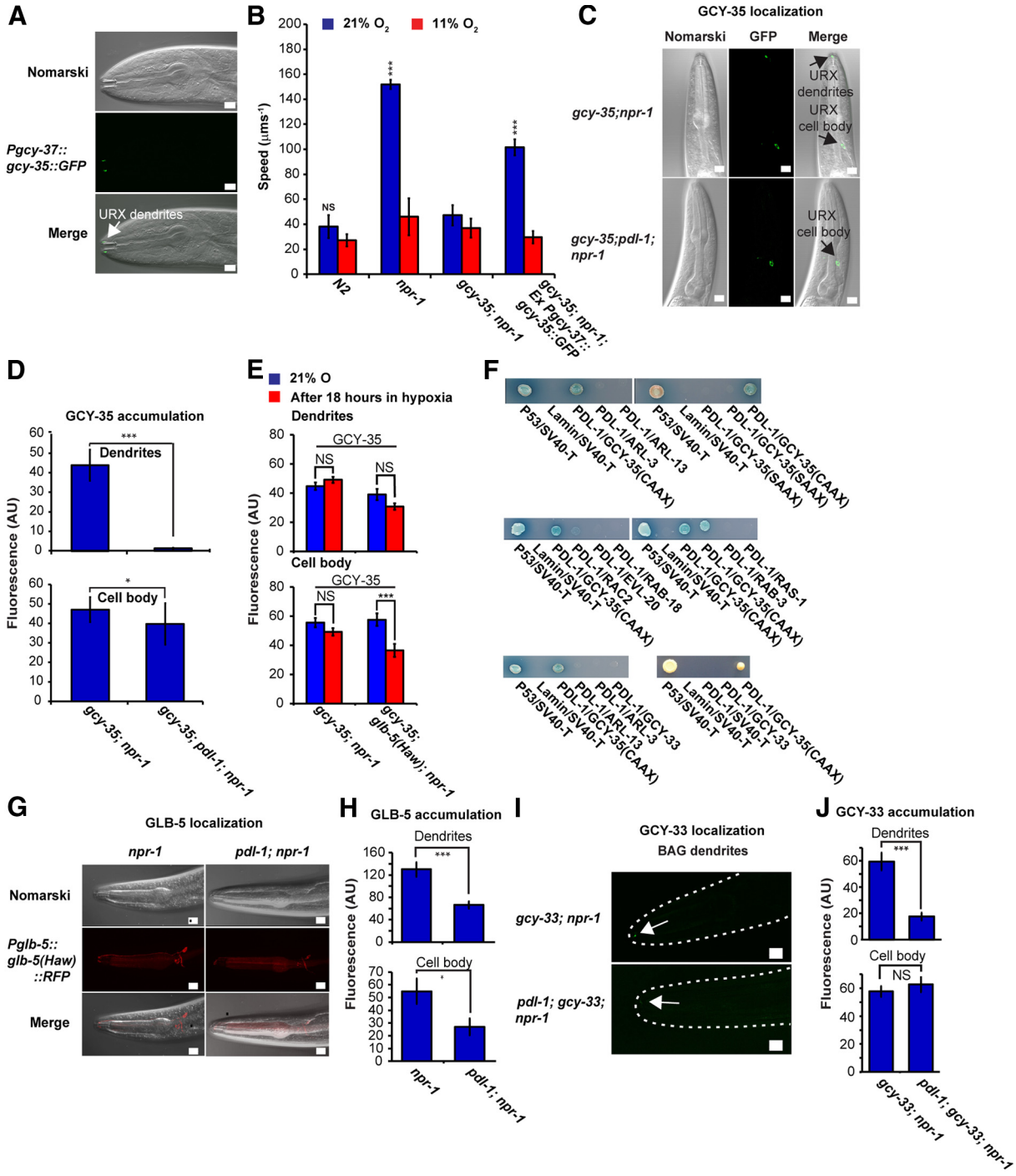

Figure 3. PDL-1 regulates GCY-35 and GCY-33 localization. ***A***, GCY-35::GFP accumulates at the dendritic tips of URX neurons. Scale bars: 10 μm. ***B***, Expressing a *gcy-35::GFP* fusion protein in the AQR, PQR, and URX neurons rescues *gcy-35; npr-1* mutant phenotypes. Asterisks indicate significant differences from *gcy-35; npr-1* animals at 21% O_2. Kruskal–Wallis test with Dunn's post-test. ***C***, PDL-1 is required for GCY-35::GFP to accumulate at the dendritic tips of URX dendrites, but not in the cell body. Scale bars: 10 μm. ***D***, Quantitation of GCY-35::GFP accumulation in dendrites and cell bodies of *gcy-35; npr-1* and *gcy-35; pdl-1; npr-1* animals; $n \geq 10$, Mann–Whitney test. ***E***, Hypoxia does not reduce GCY-35::GFP accumulation in the URX dendrites in *gcy-35; npr-1* or *gcy-35; glb-5(Haw); npr-1* animals; $n \geq 16$, Mann–Whitney test. ***F***, Yeast two-hybrid assay. Diploid growth on selectable plates containing SD/-Leu/-Trp, X-α-Gal, and Aureobasidin A. Top, PDL-1 interacts strongly with GCY-35 but not ARL-3 or ARL-13; the interactions of SV40-T with p53 and lamin provide positive and negative controls, respectively. Mutating the CAAX prenylation motif to SAAX inhibits GCY-35–PDL-1 interaction. Middle and lower left, Colonies of diploids coexpressing PDL-1 with RAC-2 or GCY-33 were much smaller compared withPDL-1::GCY-35 colonies, indicating that the interaction between these proteins and PDL-1 is weak. Supporting this, PDL-1::GCY-33 diploids did not grow on a more restrictive media (-Trp/-Leu/-Ade/-His/Aureobasidin A/X-α-Gal; lower right). ***G***, Disrupting PDL-1 reduces accumulation of mcherry-tagged GLB-5(Haw) in both dendrites and cell bodies. Scale bar, 10 μm. ***H***, Quantification of GLB-5(Haw)::mCherry fluorescence in the dendritic ending and cell body of *glb-5*-expressing head neurons in *npr-1* and *pdl-1; npr-1* animals. Data represent an average of at least 10 animals, Mann–Whitney test. ***I***, PDL-1 regulates GCY-33::GFP localization in BAG neurons. Disrupting *pdl-1* reduces accumulation of GCY-33::GFP at the tips of BAG dendrites (marked by arrows). Scale bar, 10 μm. ***J***, Quantification of GCY-33::GFP fluorescence at the dendritic ending and cell body of BAG neurons in *gcy-33; npr-1* and *pdl-1; gcy-33; npr-1* animals. Data represent an average of at least 10 animals, Mann–Whitney test. $^*p < 0.05$, $^{**}p < 0.01$, and $^{***}p < 0.001$. Error bars represent SEM.

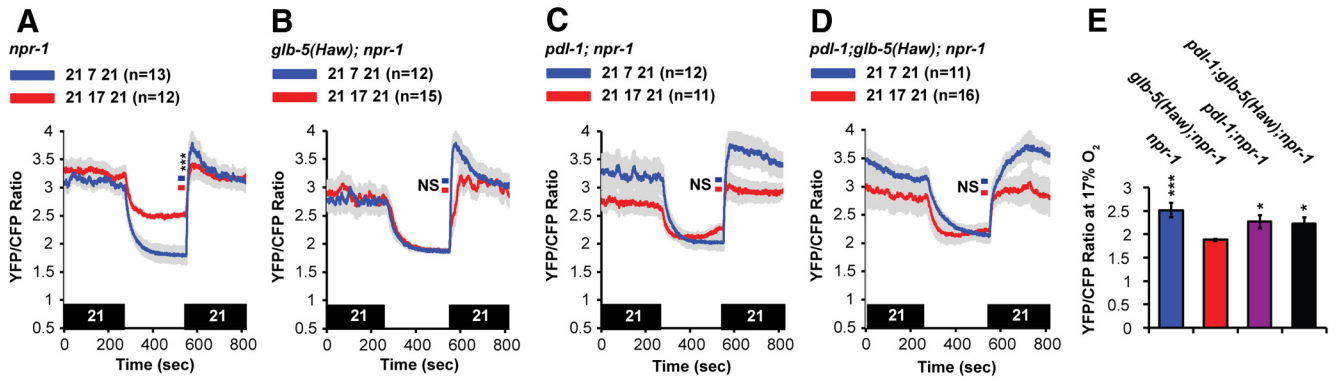

Figure 4. Disrupting PDL-1 alters O_2-evoked Ca^{2+} responses in the URX neurons. ***A–D***, Ca^{2+} responses evoked in URX by 21%–7%–21% and 21%–17%–21% O_2 stimulus trains measured using the YC2.60 sensor in *npr-1* (***A***), *glb-5(Haw); npr-1* (***B***), *pdl-1; npr-1* (***C***), and *pdl-1; glb-5(Haw); npr-1* (***D***) animals. Asterisks indicate significant differences in Ca^{2+} levels at 17 and 7% O_2 in the 30 s before the transition to 21% O_2, Mann–Whitney test. Gray shading represents SEM. ***E***, Bar graph comparing tonic URX Ca^{2+} levels at 17% O_2 in various genotypes (data taken from ***A–D***). Asterisks indicate significant differences compared with *glb-5(Haw); npr-1*. Kruskal–Wallis test with Dunn's post-test. Error bars represent SEM, $*p < 0.05$, $***p < 0.001$.

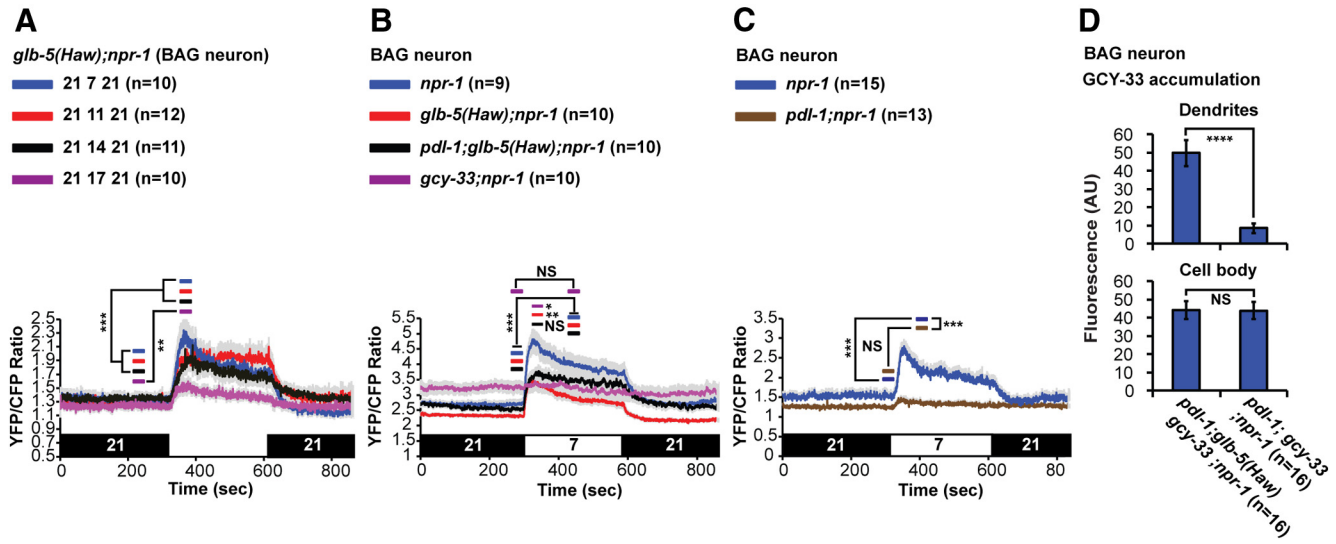

Figure 5. O_2-evoked Ca^{2+} responses in the BAG neurons. ***A***, Dynamic range of O_2-evoked responses in BAG measured using YC2.60. Asterisks indicate significant differences between Ca^{2+} levels at 21% O_2 and at the lower O_2 tension during indicated time intervals, Mann–Whitney test. ***B***, 21%–7%–21% O_2 stimulus trains evoked strong Ca^{2+} responses in BAG in *npr-1, glb-5(Haw); npr-1*, and *pdl-1; glb-5(Haw); npr-1* animals, but not in *gcy-33, npr-1* animals. Asterisks indicate significant differences for each genotype between Ca^{2+} levels at 21% O_2 and at 7% O_2 during indicated time intervals (Mann–Whitney test) or significant differences between *npr-1* and other genotypes at 7% O_2 during indicated time intervals. Kruskal–Wallis test with Dunn's post-test. ***C***, Deleting *pdl-1* attenuates O_2-evoked Ca^{2+} responses in BAG in *npr-1* animals. Asterisks indicate significant differences between *npr-1* and *pdl-1; npr-1* animals exposed to 7% O_2 at times indicated, as well as significant differences in Ca^{2+} at 21 and 7% O_2 within each strain. Mann–Whitney test. The data presented in ***B*** were collected on a different imaging setup from that used in ***A*** and ***C***. $*p < 0.05$, $**p < 0.01$, and $***p < 0.001$. Gray shading represents SEM. ***D***, GLB-5(Haw) restores localization of GCY-33-GFP to the cilia of BAG neurons in *pdl-1; gcy-33; npr-1* mutants. $****p < 0.0001$, Mann–Whitney test. Error bars represent SEM.

5(Haw); npr-1 animals (Fig. 2*D*,*F*). Our results suggest that localizing the GCY-35 O_2 sensor to the dendritic endings of URX is not essential for transducing O_2 stimuli, but that PDL-1 activity modifies O_2-evoked Ca^{2+} signaling in URX.

GLB-5 and PDL-1 modify O_2-evoked Ca^{2+} responses in BAG neurons

We next investigated how the *glb-5(Haw)* allele and *pdl-1* contributed to O_2-evoked Ca^{2+} responses in BAG neurons in normoxia-grown animals. Previous work showed that a fall in O_2 concentration evokes a rise in Ca^{2+} in BAG neurons (Zimmer et al., 2009). Our behavioral experiments suggested BAG neurons were part of the circuit that enables feeding *glb-5(Haw); npr-1* animals to reduce their locomotor activity sharply when O_2 decreases from 21 to 17% (Fig. 2*F*). To monitor BAG Ca^{2+} we expressed YC2.60 using the *flp-17* promoter. We measured Ca^{2+} changes evoked by a series of O_2 downsteps in well fed animals in the absence of food. We could detect small but robust rises in Ca^{2+} when O_2 fell from 21 to 17%; as expected Ca^{2+} responses became bigger as we reduced O_2 levels further (Fig. 5*A*). Thus, in *glb-5(Haw); npr-1* animals even small decreases in O_2 evoked an increase In BAG Ca^{2+}.

The small size of the Ca^{2+} response evoked in BAG by a switch from 21 to 17% O_2 (Fig. 5*A*) precluded us from genetically dissecting this response. Instead, we studied responses evoked by a switch from 21 to 7% O_2. As expected from previous work (Zimmer et al., 2009), O_2-evoked Ca^{2+} responses in BAG were eliminated in mutants defective in *gcy-33* (Fig. 5*B*).

To investigate how *pdl-1* modifies BAG signaling, we first compared O_2-evoked responses in *npr-1* and *pdl-1; npr-1* mutants. Disrupting *pdl-1* attenuated the rise in Ca^{2+} evoked by a switch from 21 to 7% O_2 (Fig. 5*C*). Unexpectedly, the presence of

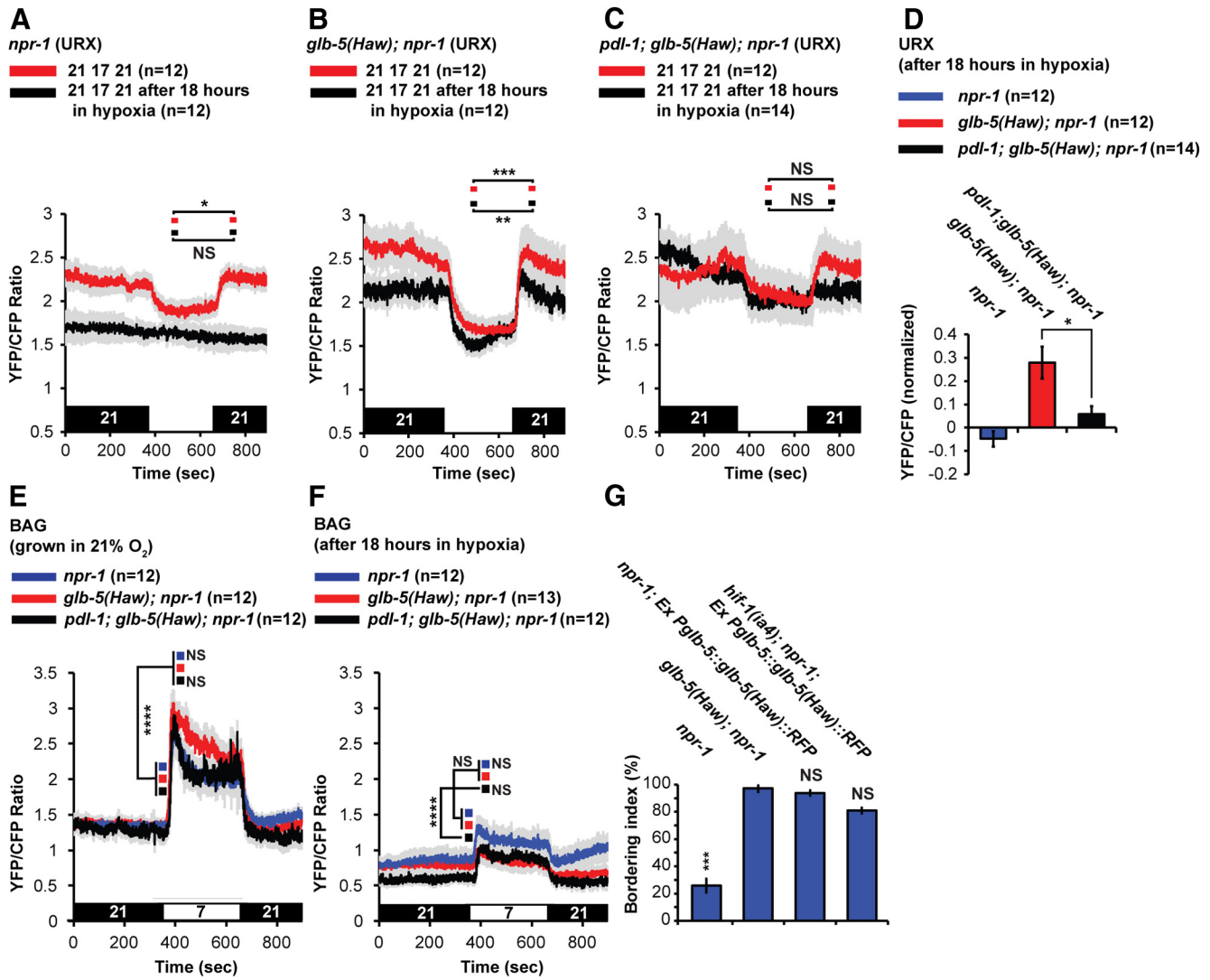

Figure 6. O_2-evoked Ca^{2+} responses in URX neurons after prolonged hypoxia. Ca^{2+} responses evoked by 21%–17%–21% O_2 stimulus trains in URX after 18 h incubation at 1% O_2 measured using YC2.60. ***A***, ***B***, Prolonged hypoxia abolishes URX responsiveness to changes in O_2 in *npr-1* animals (***A***), but has much weaker effects on *glb-5(Haw); npr-1* animals (***B***). ***C***, Deleting *pdl-1* reduced URX responsiveness of *glb-5(Haw); npr-1* animals in both normoxia and hypoxia cultivated animals, and led to higher Ca^{2+} levels at 17% O_2. ***D***, Bar graph comparing tonic URX Ca^{2+} levels at 21% O_2, just after the switch from 17% O_2 to 21% O_2, in various genotypes; data taken from ***A–C*** (21%–17%–21% O_2 responses after 18 h in hypoxia); baseline normalized ratios. Asterisks indicate significant differences compared with *glb-5(Haw); npr-1*. Mann–Whitney test, $*p < 0.05$. Error bars represent SEM. ***E***, 21%–7%–21% O_2 stimulus trains evoked strong Ca^{2+} responses in BAG in *npr-1*, *glb-5(Haw); npr-1*, and *pdl-1; glb-5(haw); npr-1* animals. ***F***, The 21%–7%–21% O_2-evoked Ca^{2+} responses in BAG were smaller after hypoxia (for comparison see ***E***). Asterisks indicate significant differences between Ca^{2+} level just after the shift from 21 to 7% O_2 at times indicated by the bars, Mann–Whitney test. Gray shading represents SEM. ***G***, Disrupting *hif-1* did not prevent the fast recovery of bordering behavior in *glb-5(Haw); npr-1* animals following exposure to hypoxia. Asterisks indicate significance for comparisons with *glb-5(Haw); npr-1* animals. Kruskal–Wallis test with Dunn's post-test, $n \geq 4$, $*p < 0.05$, $**p < 0.01$, and $***p < 0.001$. Error bars represent SEM.

GLB-5(Haw) compensated for the loss of *pdl-1*; Ca^{2+} responses evoked by a 21–7% O_2 stimulus in *pdl-1; glb-5(Haw); npr-1* and *glb-5(Haw); npr-1* animals were similar (Fig. 5*B*). Why? If the BAG response defect in *pdl-1; npr-1* animals reflected loss of GCY-33 localization to cilia, then GLB-5(Haw) should rescue not only the Ca^{2+} response of *pdl-1; npr-1* animals, but also the GCY-33 localization defect. This is in fact the case: GLB-5(Haw) restored GCY-33 accumulation at the dendritic endings of BAG to *pdl-1; npr-1* animals, without affecting GCY-33 levels in the cell body (Fig. 5*D*). Together, our results suggest that GCY-33 localization at the dendritic-endings of BAG is important for BAG O_2 sensing. Moreover, since GLB-5(Haw) is involved in GCY-33 trafficking to or retention in cilia, our data suggest that GLB-5 and GCY-33 are part of a complex *in vivo*.

Hypoxia modifies O_2-sensor physiology

Having explored how GLB-5(Haw) and PDL-1 activity shaped the O_2 responses of BAG and URX neurons in animals grown in normoxia, we explored how these genes influenced the physiology of O_2-sensing neurons after hypoxia experience. We kept animals in 1% O_2 for 18 h and then imaged O_2-evoked Ca^{2+} responses. For these experiments, individual worms were transferred from the hypoxia chamber and rapidly glued to agarose pads in a 21% O_2 environment. All experiments were done in the presence of food as described previously, and begun within 5 min from the time of transfer. For URX, we chose a 21%–17%–21% O_2 stimulus train to evoke neuronal activity, since it mimics the O_2 concentration difference between the bacterial lawn (~17% O_2) and the surrounding agar (~21% O_2) in the bordering assay plates. Ca^{2+}

responses were undetectable in *npr-1* animals following hypoxic cultivation (Fig. 6*A*). In contrast, *glb-5(Haw); npr-1* animals retained strong O_2-evoked Ca^{2+} responses in URX after exposure to hypoxia (Fig. 6*B*). These data suggest that hypoxia/re-oxygenation reconfigures the activity of URX in *npr-1* animals, and that the *glb-5(Haw)* allele either suppresses this reconfiguration or enables rapid recovery. In hypoxia-conditioned *pdl-1; glb-5(Haw); npr-1* animals, URX neurons responded less robustly than *glb-5(Haw); npr-1* controls to O_2 stimuli (Fig. 6*C*,*D*), suggesting that the protective effect of GLB-5(Haw) is partly dependent on PDL-1. These imaging results are consistent with our behavioral observations that hypoxia experience inhibits bordering in *npr-1* and *pdl-1; glb-5(Haw); npr-1* but not *glb-5(Haw); npr-1* animals (Fig. 2*A*, *C*).

To explore if the physiology of BAG neurons was also reconfigured by hypoxia, we compared O_2-evoked Ca^{2+} responses in animals kept for 18 h at 21% or 1% O_2 (Fig. 6*E*,*F*). The 21%–7%–21% O_2 stimulus trains elicited smaller Ca^{2+} responses in *npr-1* and *glb-5(Haw); npr-1* animals after exposure to hypoxia (Fig. 6*E*,*F*). These results suggest that like in URX, hypoxia experience reconfigures BAG O_2 responses; however, unlike in URX, the presence of GLB-5(Haw) or absence of PDL-1 did not appear to have strong effects. One caveat is that expression of the YC2.60 sensor in BAG neurons was decreased in hypoxia-treated animals, complicating comparisons across O_2 conditions.

GLB-5(Haw) suppresses behavioral reconfiguration by hypoxia in an HIF-1-independent mechanism

The reconfiguration of bordering behavior by hypoxia occurred over hours (Fig. 1*B*), suggesting that transcriptional regulation is involved. Since HIF-1 is a key factor in adaptation to hypoxia (Semenza and Wang, 1992; Jiang et al., 2001), we wondered if HIF-1 was involved. To test this, we examined the bordering behavior of *hif-1(ia4); npr-1; pglb-5:glb-5(Haw)* animals after hypoxia (Fig. 6*G*). *hif-1(ia4)* animals survived well in 24 h hypoxia, and upon exposure to 1% O_2, left food and accumulated outside the bacteria. When returned to 21% O_2, *hif-1(ia4); npr-1; pglb-5:glb-5(Haw)* animals rapidly resumed bordering behavior, like *glb-5(Haw); npr-1* animals. These results suggest that HIF-1 is not required for GLB-5(Haw) to promote rapid recovery from hypoxia exposure, although we have not examined if it required for *npr-1* animals to inhibit bordering following hypoxia experience.

GLB-5(Haw) enables URX neurons adapted to hypoxia to rapidly retune their O_2 response set point upon return to normoxia

GLB-5(Haw) counteracts the effects of prolonged hypoxia on behavior and URX physiology after animals are returned to normoxia. We speculated that GLB-5 could do this in one of two ways: by preventing hypoxia from reconfiguring the physiology of URX or by enabling rapid recovery of URX response properties when animals exposed to prolonged hypoxia are returned to 21% O_2. In the second model URX recovery would need to be fast, since *glb-5(Haw); npr-1* animals showed substantial O_2-evoked Ca^{2+} responses within 5 min of transfer from hypoxia to 21% O_2 (Fig. 6*B*).

To differentiate between these possibilities we built an airtight microfluidic-imaging chamber that enabled us to measure URX response properties in hypoxia-grown animals without prior exposure to 21% O_2. Since gluing animals in the hypoxia chamber was difficult, we immobilized animals using the cholinergic agonist levamisole (see Materials and Methods). We grew *npr-1* and *glb-5(Haw); npr-1* animals for 18 h in either 1% or 21% O_2, transferred them to the imaging scope, and shifted them from 1 to 7% O_2. To compare the effects of acute and prolonged hypoxia, we also exposed *npr-1* and *glb-5(Haw); npr-1* animals cultivated at 21% O_2 to a 21%–1%–7–21% O_2 stimulus train. Animals adapted to 1% O_2 for 18 h exhibited large persistent increases in URX Ca^{2+} when shifted to 7% O_2 (Fig. 7*A*,*B*), whereas animals exposed to 1% O_2 for only 5 min exhibited a smaller, transient increase in Ca^{2+} to the same 7% O_2 stimulus (Fig. 7*C*–*E*). The effects of prolonged hypoxia on URX activity after O_2 levels were raised for the first time from 1 to 7% were independent of GLB-5(Haw) activity (Fig. 7*A*,*B*). This contrasts with the marked difference in O_2-evoked Ca^{2+} responses in URX when hypoxia-treated *npr-1* and *glb-5(Haw); npr-1* animals were exposed to 21% O_2 (Fig. 6*A*,*B*). These data suggest that hypoxia can reprogram URX activity in both *npr-1* and *glb-5(Haw); npr-1* animals, but that recovery after further exposure to 21% O_2 is much faster in *glb-5(Haw); npr-1* than *npr-1* animals.

Discussion

The neuroglobin GLB-5(Haw) enables fast behavioral recovery after exposure to hypoxia. At 21% O_2 wild *C. elegans* rapidly accumulate where bacterial food is thickest. This foraging behavior, called bordering, is inhibited by prior hypoxia experience if *glb-5* is defective. The effects of hypoxia exposure on subsequent behavior at 21% O_2 build up gradually and plateau after 18 h in 1% O_2. *C. elegans* relies on the URX O_2-sensing neurons to accumulate where bacteria are thickest; these neurons are activated by a rise in O_2. If GLB-5 is defective, prolonged hypoxia and re-oxygenation disrupts O_2-evoked Ca^{2+} responses of URX neurons. A simple hypothesis is that GLB-5 mitigates the effects of hypoxia/re-oxygenation by controlling O_2-evoked Ca^{2+} dynamics during this transition. The exact molecular mechanism by which this is achieved is unclear, but GLB-5, like many other hexacoordinated globins, oxidizes rapidly in 21% O_2 (Persson et al., 2009; Yoon et al., 2010), making it a potential electron donor that signals by generating reactive oxygen species.

GLB-5(Haw)'s ability to promote rapid recovery of bordering after hypoxia experience, and to tune URX neurons to changes in O_2 between 21 and 17%, depend on PDL-1, the *C. elegans* ortholog of the mammalian prenyl binding protein PDEδ. PDL-1 is required in both the URX and BAG neurons to sustain these GLB-5(Haw)-dependent behaviors. BAG, like URX, is an O_2 sensor, but is activated by a decrease instead of an increase in O_2 due to the activity of the GCY-33/GCY-31soluble guanylate cyclase (Zimmer et al., 2009). PDL-1 mediates GCY-35 and GCY-33 O_2 sensor localization to the dendritic endings of URX and BAG neurons, respectively (Fig. 3*C*,*I*). Since GLB-5 is also localized to the dendritic endings of URX, one interpretation of our data is that physical proximity helps GLB-5 modify O_2 sensory transduction by GCY-35/GCY-36. In BAG neurons GCY-33 and GLB-5 likely function in a complex, since GLB-5(Haw) can target GCY-33 to cilia in the absence of PDL-1. Although a simple model in which the effects of PDL-1 are mediated via localization of soluble guanylate cyclase is appealing, PDL-1 may play a more complex role involving trafficking of other prenylated proteins. For example, in mammals PDEδ traffics heterotrimeric guanine-nucleotide binding protein gamma subunits; the *C. elegans* orthologs of these genes, *gpc-1* and *gpc-2*, are also predicted to be prenylated.

PDL-1 activity is required in BAG for GLB-5(Haw) to confer a strong behavioral response to switches between 21% and 17% O_2 (Fig. 2*F*). Consistent with this, a 21%–17%–21% O_2 stimulus

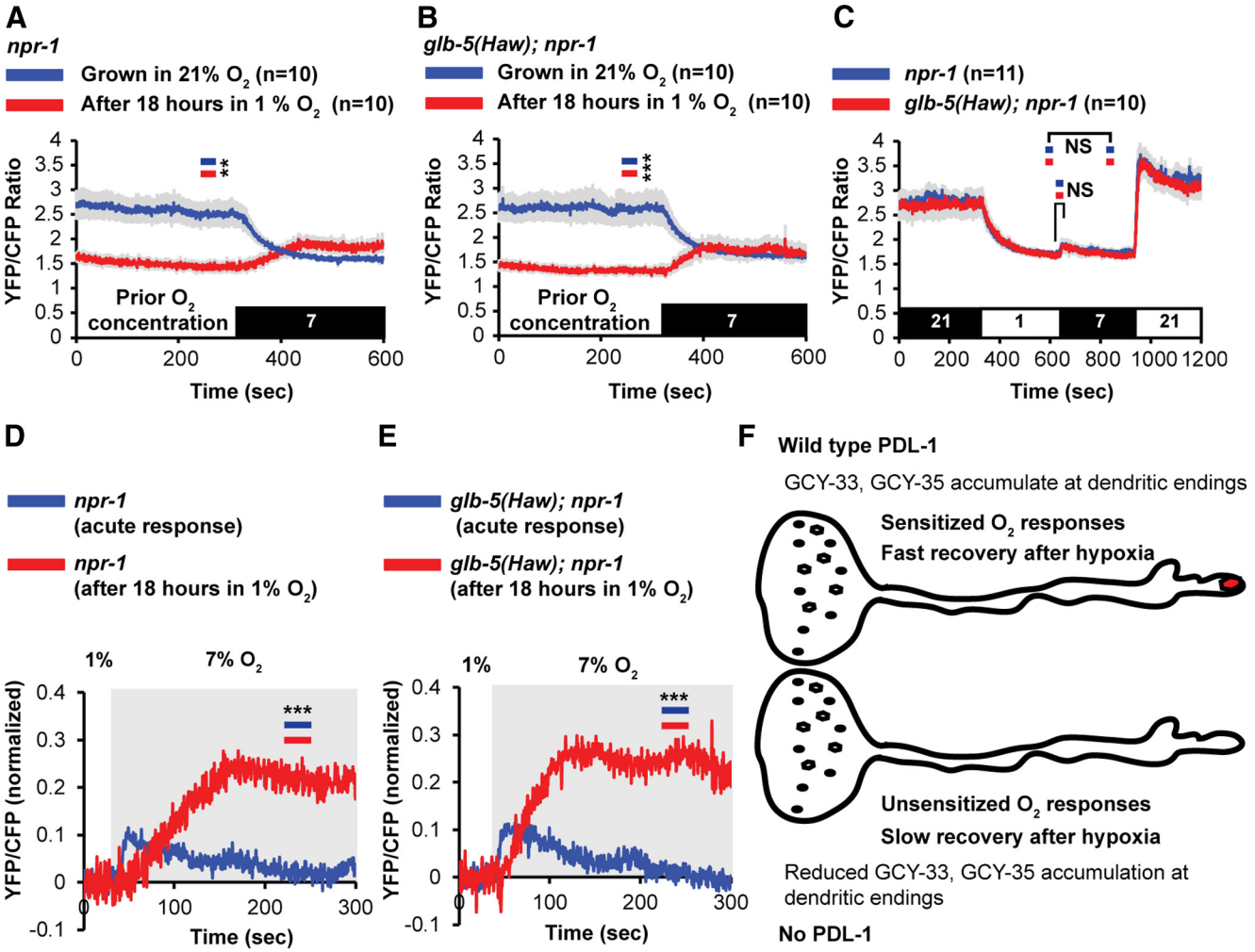

Figure 7. Prolonged hypoxia reconfigures URX O_2 responses in *npr-1* and *glb-5(Haw); npr-1* animals. ***A***, B. Ca^{2+} responses evoked in URX by 7% O_2 after 18 h incubation in 1% O_2. The Ca^{2+} sensor is YC2.60. Animals that were incubated in 1% O_2 did not experience 21% O_2 before the 7% O_2 stimulus. The transition from hypoxia to 7% O_2 elicited an increase in Ca^{2+} in *npr-1* and *glb-5(Haw); npr-1* animals. Asterisks indicate significant differences at times indicated by bars between the Ca^{2+} levels before the transition to 7% O_2, Mann–Whitney test. ***C***, Brief exposure to 1% O_2 followed by a 7% O_2 stimulus did not elicit a strong and enduring increase in Ca^{2+} concentration in *npr-1* and *glb-5(Haw); npr-1* animals. Asterisks indicate significant differences compared with the Ca^{2+} level in 1% O_2, at times indicated by bars just before the transition to 7% O_2, Mann–Whitney test. ***D***, ***E***, Prolonged exposure to hypoxia reconfigures URX O_2 responses. A comparison of responses evoked by a switch from 1 to 7% O_2 in *npr-1* and *glb-5(Haw); npr-1* animals (from ***A*** and ***C***; ***B*** and ***C***, baseline normalized ratios). Asterisks indicate significant differences compared with the Ca^{2+} level in 1% O_2 after 3 min in 7% O_2. Mann–Whitney test, $*p < 0.05$, $**p < 0.01$, and $***p < 0.001$. Gray shading represents SEM. ***F***, Model for PDL-1 activity in the URX and BAG neurons. Prenylated GCY-33 and GCY-35 interact with PDL-1, which facilitates their traffic to dendritic endings. There, they act together with GLB-5(Haw) to tune the dynamic range of O_2 responses, and to rapidly retune O_2-sensing properties after return to normoxia following prolonged hypoxia.

train evoked a significant rise and fall in Ca^{2+} levels in BAG in well fed *glb-5(Haw); npr-1* animals (Fig. 5). Thus, the same small changes in ambient O_2 concentration induce reciprocal O_2 responses in URX and BAG, and act antagonistically to control locomotor activity: at 21% O_2 high URX/low BAG activity promotes rapid movement, whereas at 17% O_2 low URX/high BAG activity promotes slow movement (Figs. 4, 5). Previous work has already demonstrated reciprocal O_2 responses in URX and BAG, but BAG responses in those studies were evoked at much lower O_2 concentrations (Zimmer et al., 2009). Like URX, BAG neurons appear to have tonic signaling activity, since BAG Ca^{2+} levels remained elevated while O_2 levels were reduced. Consistent with our data, previous work has shown that activating BAG induces animals to reduce locomotor activity (Zimmer et al., 2009).

PDE6δ is considered to be a promiscuous prenyl binding protein (Zhang et al., 2004). However, in our yeast two-hybrid assays PDL-1 did not interact with several well known prenylated proteins such as RAS-1 and RAB-18, or ARL2-like proteins such as ARL-3 and EVL-20 (Fig. 3*F*). Moreover, the interaction of PDL-1 with GCY-33 was significantly weaker than its interaction with GCY-35 in the same assay. One explanation is that expression of these prenylated proteins in yeast is variable. An alternative explanation is that the substrate specificity of PDL-1 for prenylated proteins is complex.

The neuronal functions of mammalian PDE6δ have been previously studied in rods and cones, where it regulates transport of phosphodiesterase PDE6, rhodopsin kinase, and $G_{t\alpha}$—all prenylated proteins—to the outer segment of these ciliated neurons (Li et al., 1998; Norton et al., 2005; Zhang et al., 2007; Luo et al., 2008). Like cone and rod photoreceptors, BAG has a ciliated dendritic ending, but URX is a nonciliated neuron (Ward et al., 1975). Thus, prenyl binding proteins can facilitate protein traffic to both ciliated and nonciliated dendritic endings. The localization of GCY-35 and GCY-33 may regulate O_2 sensory transduction level in two ways. First, localization of these molecular O_2 sensors probably alters their O_2 environment: the dendritic end-

ings of URX and BAG are located close to the surface at the *C. elegans* nose tip, where O_2 concentrations are likely to be higher than those found in the cell bodies, which lie buried inside the animal. Second, as highlighted above, components of the O_2 sensory transduction machinery, including GLB-5 (Persson et al., 2009) and cGMP-gated channels (Arellano-Carbajal et al., 2011), are enriched at the dendritic endings of URX, facilitating compartmentalized signaling. Interestingly, although *pdl-1* mutants have little detectable GCY-35 at URX dendritic endings, they retain strong O_2-evoked Ca^{2+} responses in these neurons, indicating that cGMP signal transduction can still function. This suggests that soluble guanylate cyclases and cGMP channels remain in close proximity in *pdl-1* mutants.

Prolonged hypoxia reconfigures responses to O_2 in other *C. elegans* behavioral paradigms, although the role of globins was not studied (Cheung et al., 2005; Chang and Bargmann, 2008; Ma et al., 2012). Our Ca^{2+} imaging experiments demonstrate that previous O_2 experience can retune URX O_2 responses (Fig. 7*A*,*B*). Interestingly, previous studies of HIF-1 activation showed that the HT22 mouse neuronal cell line and cardiofibroblasts can adjust their O_2 sensitivity in response to prolonged incubation in 5% or 30% O_2 (Roy et al., 2003; Khanna et al., 2006). Prolonged exposure of HT22 cells to 5% O_2 attenuates subsequent HIF-1 activation by 0.5% O_2. Moreover, HIF-1 activity increases when HT22 cells grown in 30% O_2 are transferred to 20% O_2. These studies suggest that in these cells the O_2 balance point for HIF-1 induction is regulated by experience.

In summary, our results suggest that the GLB-5 neuroglobin confers on *C. elegans* O_2 sensors the ability to retain their tuning properties following prolonged hypoxia and re-oxygenation. This mechanism allows fast behavioral and cellular activity adjustment following re-oxygenation. It would be interesting to test if mammalian neuroglobin regulates the threshold for O_2 responses in glomus cells of the carotid body (Di Giulio et al., 2006, 2012). Our results also suggest that PDL-1, the *C. elegans* ortholog of PDEδ, facilitates traffic of prenylated GCY-35 and GCY-33 from the cell bodies of BAG and URX neurons to their ciliated and nonciliated dendritic endings, respectively. PDL-1 is highly conserved between *C. elegans* and humans, plays a major role in vision physiology, and spatially regulates K-RAS activity in human cells (Zhang et al., 2012; Zimmermann et al., 2013). Our studies establish a tractable *in vivo* system to study PDL-1 function *in vivo*, enabling its mechanisms of action to be explored further and potential small molecule inhibitors to be tested.

References

Abramoff MD, Magelhaes PJ, Ram SJ (2004) Image processing with ImageJ. Biophot Int 11:36–42.

Arellano-Carbajal F, Briseño-Roa L, Couto A, Cheung BH, Labouesse M, de Bono M (2011) Macoilin, a conserved nervous system-specific ER membrane protein that regulates neuronal excitability. PLoS Genet 7:e1001341. CrossRef Medline

Brenner S (1974) The genetics of *Caenorhabditis elegans*. Genetics 77:71–94. Medline

Burmester T, Hankeln T (2009) What is the function of neuroglobin? J Exp Biol 212:1423–1428. CrossRef Medline

Busch KE, Laurent P, Soltesz Z, Murphy RJ, Faivre O, Hedwig B, Thomas M, Smith HL, de Bono M (2012) Tonic signaling from O(2) sensors sets neural circuit activity and behavioral state. Nat Neurosci 15:581–591. CrossRef Medline

Chandra A, Grecco HE, Pisupati V, Perera D, Cassidy L, Skoulidis F, Ismail SA, Hedberg C, Hanzal-Bayer M, Venkitaraman AR, Wittinghofer A, Bastiaens PI (2012) The GDI-like solubilizing factor PDEdelta sustains the spatial organization and signalling of Ras family proteins. Nat Cell Biol 14:148–158. Medline

Chang AJ, Bargmann CI (2008) Hypoxia and the HIF-1 transcriptional pathway reorganize a neuronal circuit for oxygen-dependent behavior in *Caenorhabditis elegans*. Proc Natl Acad Sci U S A 105:7321–7326. CrossRef Medline

Cheung BH, Arellano-Carbajal F, Rybicki I, de Bono M (2004) Soluble guanylate cyclases act in neurons exposed to the body fluid to promote *C. elegans* aggregation behavior. Curr Biol 14:1105–1111. CrossRef Medline

Cheung BH, Cohen M, Rogers C, Albayram O, de Bono M (2005) Experience-dependent modulation of *C. elegans* behavior by ambient oxygen. Curr Biol 15:905–917. CrossRef Medline

Coates JC, de Bono M (2002) Antagonistic pathways in neurons exposed to body fluid regulate social feeding in *Caenorhabditis elegans*. Nature 419:925–929. CrossRef Medline

Couto A, Oda S, Nikolaev VO, Soltesz Z, de Bono M (2013) In vivo genetic dissection of O2-evoked cGMP dynamics in a *Caenorhabditis elegans* gas sensor. Proc Natl Acad Sci U S A 110:E3301–E3310. CrossRef Medline

Davis MW, Hammarlund M, Harrach T, Hullett P, Olsen S, Jorgensen EM (2005) Rapid single nucleotide polymorphism mapping in *C. elegans*. BMC Genomics 6:118. CrossRef Medline

de Bono M, Bargmann CI (1998) Natural variation in a neuropeptide Y receptor homolog modifies social behavior and food response in *C. elegans*. Cell 94:679–689. CrossRef Medline

Di Giulio C, Bianchi G, Cacchio M, Artese L, Piccirilli M, Verratti V, Valerio R, Iturriaga R (2006) Neuroglobin, a new oxygen binding protein is present in the carotid body and increases after chronic intermittent hypoxia. Adv Exp Med Biol 580:15–19; discussion 351–359. CrossRef Medline

Di Giulio C, Zara S, Cataldi A, Porzionato A, Pokorski M, De Caro R (2012) Human carotid body HIF and NGB expression during human development and aging. Adv Exp Med Biol 758:265–271. CrossRef Medline

Esposito G, Di Schiavi E, Bergamasco C, Bazzicalupo P (2007) Efficient and cell specific knock-down of gene function in targeted *C. elegans* neurons. Gene 395:170–176. CrossRef Medline

Gillespie PG, Prusti RK, Apel ED, Beavo JA (1989) A soluble form of bovine rod photoreceptor phosphodiesterase has a novel 15-kDa subunit. J Biol Chem 264:12187–12193. Medline

Gray JM, Karow DS, Lu H, Chang AJ, Chang JS, Ellis RE, Marletta MA, Bargmann CI (2004) Oxygen sensation and social feeding mediated by a *C. elegans* guanylate cyclase homologue. Nature 430:317–322. CrossRef Medline

Hanzal-Bayer M, Renault L, Roversi P, Wittinghofer A, Hillig RC (2002) The complex of Arl2-GTP and PDE delta: from structure to function. EMBO J 21:2095–2106. CrossRef Medline

Hoogewijs D, Geuens E, Dewilde S, Vierstraete A, Moens L, Vinogradov S, Vanfleteren JR (2007) Wide diversity in structure and expression profiles among members of the *Caenorhabditis elegans* globin protein family. BMC Genomics 8:356. CrossRef Medline

Hundahl CA, Kelsen J, Hay-Schmidt A (2013) Neuroglobin and Cytoglobin expression in the human brain. Brain Struct Funct 218:603–609. CrossRef Medline

Jiang H, Guo R, Powell-Coffman JA (2001) The *Caenorhabditis elegans* hif-1 gene encodes a bHLH-PAS protein that is required for adaptation to hypoxia. Proc Natl Acad Sci U S A 98:7916–7921. CrossRef Medline

Khanna S, Roy S, Maurer M, Ratan RR, Sen CK (2006) Oxygen-sensitive reset of hypoxia-inducible factor transactivation response: prolyl hydroxylases tune the biological normoxic set point. Free Radic Biol Med 40:2147–2154. CrossRef Medline

Kiontke KC, Félix MA, Ailion M, Rockman MV, Braendle C, Pénigault JB, Fitch DH (2011) A phylogeny and molecular barcodes for Caenorhabditis, with numerous new species from rotting fruits. BMC Evol Biol 11:339. CrossRef Medline

Kozarewa I, Ning Z, Quail MA, Sanders MJ, Berriman M, Turner DJ (2009) Amplification-free Illumina sequencing-library preparation facilitates improved mapping and assembly of (G+C)-biased genomes. Nat Methods 6:291–295. CrossRef Medline

Li N, Florio SK, Pettenati MJ, Rao PN, Beavo JA, Baehr W (1998) Characterization of human and mouse rod cGMP phosphodiesterase delta subunit (PDE6D) and chromosomal localization of the human gene. Genomics 49:76–82. CrossRef Medline

Luo DG, Xue T, Yau KW (2008) How vision begins: an odyssey. Proc Natl Acad Sci U S A 105:9855–9862. CrossRef Medline

Ma DK, Vozdek R, Bhatla N, Horvitz HR (2012) CYSL-1 interacts with the

O2-sensing hydroxylase EGL-9 to promote H2S-modulated hypoxia-induced behavioral plasticity in *C. elegans*. Neuron 73:925–940. CrossRef Medline

McGrath PT, Rockman MV, Zimmer M, Jang H, Macosko EZ, Kruglyak L, Bargmann CI (2009) Quantitative mapping of a digenic behavioral trait implicates globin variation in *C. elegans* sensory behaviors. Neuron 61: 692–699. CrossRef Medline

Mello CC, Kramer JM, Stinchcomb D, Ambros V (1991) Efficient gene transfer in *C. elegans*: extrachromosomal maintenance and integration of transforming sequences. EMBO J 10:3959–3970. Medline

Nagai T, Yamada S, Tominaga T, Ichikawa M, Miyawaki A (2004) Expanded dynamic range of fluorescent indicators for Ca(2+) by circularly permuted yellow fluorescent proteins. Proc Natl Acad Sci U S A 101: 10554–10559. CrossRef Medline

Norton AW, Hosier S, Terew JM, Li N, Dhingra A, Vardi N, Baehr W, Cote RH (2005) Evaluation of the 17-kDa prenyl-binding protein as a regulatory protein for phototransduction in retinal photoreceptors. J Biol Chem 280:1248–1256. CrossRef Medline

Persson A, Gross E, Laurent P, Busch KE, Bretes H, de Bono M (2009) Natural variation in a neural globin tunes oxygen sensing in wild *Caenorhabditis elegans*. Nature 458:1030–1033. CrossRef Medline

Rockman MV, Kruglyak L (2009) Recombinational landscape and population genomics of *Caenorhabditis elegans*. PLoS Genet 5:e1000419. CrossRef Medline

Roy S, Khanna S, Wallace WA, Lappalainen J, Rink C, Cardounel AJ, Zweier JL, Sen CK (2003) Characterization of perceived hyperoxia in isolated primary cardiac fibroblasts and in the reoxygenated heart. J Biol Chem 278:47129–47135. CrossRef Medline

Sambrook J, Fritsch EF, Maniatis T (1989) Molecular cloning: a laboratory manual, Ed 2. New York: Cold Spring Harbor Laboratory.

Sarin S, Prabhu S, O'Meara MM, Pe'er I, Hobert O (2008) *Caenorhabditis elegans* mutant allele identification by whole-genome sequencing. Nat Methods 5:865–867. CrossRef Medline

Semenza GL, Wang GL (1992) A nuclear factor induced by hypoxia via de novo protein synthesis binds to the human erythropoietin gene enhancer at a site required for transcriptional activation. Mol Cell Biol 12:5447–5454. Medline

Sun Y, Jin K, Mao XO, Zhu Y, Greenberg DA (2001) Neuroglobin is up-regulated by and protects neurons from hypoxic-ischemic injury. Proc Natl Acad Sci U S A 98:15306–15311. CrossRef Medline

Van Voorhies WA, Ward S (2000) Broad oxygen tolerance in the nematode *Caenorhabditis elegans*. J Exp Biol 203:2467–2478. Medline

Ward JP (2008) Oxygen sensors in context. Biochim Biophys Acta 1777:1–14. CrossRef Medline

Ward S, Thomson N, White JG, Brenner S (1975) Electron microscopical reconstruction of the anterior sensory anatomy of the nematode *Caenorhabditis elegans*.?2UU. J Comp Neurol 160:313–337. CrossRef Medline

Weber KP, De S, Kozarewa I, Turner DJ, Babu MM, de Bono M (2010) Whole genome sequencing highlights genetic changes associated with laboratory domestication of *C. elegans*. PLoS One 5:e13922. CrossRef Medline

Wicks SR, Yeh RT, Gish WR, Waterston RH, Plasterk RH (2001) Rapid gene mapping in *Caenorhabditis elegans* using a high density polymorphism map. Nat Genet 28:160–164. CrossRef Medline

Yoon J, Herzik MA Jr, Winter MB, Tran R, Olea C Jr, Marletta MA (2010) Structure and properties of a bis-histidyl ligated globin from *Caenorhabditis elegans*. Biochemistry 49:5662–5670. CrossRef Medline

Zhang H, Liu XH, Zhang K, Chen CK, Frederick JM, Prestwich GD, Baehr W (2004) Photoreceptor cGMP phosphodiesterase delta subunit (PDEdelta) functions as a prenyl-binding protein. J Biol Chem 279:407–413. CrossRef Medline

Zhang H, Li S, Doan T, Rieke F, Detwiler PB, Frederick JM, Baehr W (2007) Deletion of PrBP/delta impedes transport of GRK1 and PDE6 catalytic subunits to photoreceptor outer segments. Proc Natl Acad Sci U S A 104: 8857–8862. CrossRef Medline

Zhang H, Constantine R, Frederick JM, Baehr W (2012) The prenyl-binding protein PrBP/delta: a chaperone participating in intracellular trafficking. Vision Res 75:19–25. CrossRef Medline

Zimmer M, Gray JM, Pokala N, Chang AJ, Karow DS, Marletta MA, Hudson ML, Morton DB, Chronis N, Bargmann CI (2009) Neurons detect increases and decreases in oxygen levels using distinct guanylate cyclases. Neuron 61:865–879. CrossRef Medline

Zimmermann G, Papke B, Ismail S, Vartak N, Chandra A, Hoffmann M, Hahn SA, Triola G, Wittinghofer A, Bastiaens PI, Waldmann H (2013) Small molecule inhibition of the KRAS-PDEdelta interaction impairs oncogenic KRAS signalling. Nature 497:638–642. CrossRef Medline